Numerical Modelling of ICRF Physics Experiments in the Alcator C-Mod Tokamak*

P.T. Bonoli, R.L. Boivin, M. Brambilla 1), C.L. Fiore, J.A. Goetz, R.S. Granetz, M.J. Greenwald, A.E. Hubbard, I.H. Hutchinson, J.H. Irby, B. LaBombard, W. Davis Lee, B. Lipschultz, E.S. Marmar, A. Mazurenko, E. Nelson-Melby, D. Mossessian, C.K. Phillips 2), M. Porkolab, J.E. Rice, G. Schilling 2), J.A. Snipes, J.L. Terry, S.M. Wolfe, S. J. Wukitch, and the ALCATOR GROUP

MIT Plasma Science and Fusion Center, Cambridge, Massachusetts, USA
1) Max Planck Institut für Plasmaphysik, Garching, Germany
2) Princeton Plasma Physics Laboratory, Princeton, NJ, USA

e-mail: bonoli@psfc.mit.edu

Abstract. A full-wave spectral code (TORIC) has been used to simulate mode converted ion Bernstein wave (IBW) propagation and absorption for the first time at high poloidal mode number ($-80 \lesssim m \lesssim +80$). Converged wave solutions for the mode converted wave are obtained in this limit and the predicted electron damping of the IBW is found to be consistent with experimental measurements from the Alcator C-Mod tokamak. The TORIC code has also been coupled to a bounce-averaged Fokker Planck module FPPRF and the combined codes are now run within the transport analysis tool TRANSP. This model was used to analyze off-axis hydrogen minority heating experiments in C-Mod where an internal transport barrier was obtained.

1. Introduction.

Alcator C-Mod is a compact ($R_0 = 0.67$ m, $a = 0.22$ m), high density, high magnetic field tokamak [1] operating with ion cyclotron resonance heating (ICRH) as its sole source of auxiliary heating. The wide range in operating density and magnetic field ($n_e \simeq 0.5 - 5.0 \times 10^{20}$ m^{-3} and $B_0 \simeq 2.5 - 8.0$ T) combined with the available rf source power, allow a variety of ICRF heating and mode conversion schemes to be tested on C-Mod. The present ICRF system consists of 4 MW of tunable (40-80 MHz) source power coupled through a phaseable, four strap antenna array and 4 MW of fixed frequency (80 MHz) source power coupled through two separate dipole antennas. At 80 MHz, minority ion heating regimes can be accessed in D(H) plasmas at $B_0 \simeq 4.4 - 6.0$ T and ^{3}He minority heating can be explored at 7.0 - 7.9 T. Off -axis ($r/a \gtrsim 0.5$) mode conversion electron heating (MCEH) can also be performed at $B_0 \simeq 7.9T$ and for $n_{^3\mathrm{He}}/n_e \gtrsim 0.10$. Mode conversion current drive (MCCD) experiments are also planned for C-Mod using the four strap antenna driven at 60 MHz in D(^{3}He) plasmas at $B_0 \simeq 5.5 - 6.0$ T.

In order to understand better the underlying rf physics of these experiments and prepare for future experiments, we have implemented two sophisticated simulation models for ICRF heating. The first is a full-wave ICRF code (TORIC) [2,3] which employs a poloidal mode representation for the wave electric field of the form:

$$\vec{E} = \sum_{m,n_\phi} \vec{\hat{E}}_{m,n_\phi}(r)\, \exp(im\theta + in_\phi\phi), \tag{1}$$

where m and n_ϕ are respectively the poloidal and toroidal mode numbers. Typically 240 -480 elements are retained in the radial direction. A limited number of poloidal modes

($N_{\rm m} \simeq 32$) is used to simulate minority heating and up to 161 poloidal modes have been retained to simulate properly mode conversion electron heating and current drive. These computations are described in more detail in Sec. 2. To carry out meaningful transport analysis of ICRF-heated plasmas in C-Mod it is necessary to compute the electron and ion heating profiles of the incident fast wave ICRF power. This was accomplished by coupling the TORIC code to a bounce-averaged Fokker Planck module FPPRF [4]. The combined codes are run within the transport analysis tool TRANSP [5]. Detailed results from this model will be presented in Sec. 3 for an internal transport barrier (ITB) mode that was obtained in C-Mod with off-axis hydrogen minority heating at 4.5 T.

2. Mode Conversion Electron Heating: Simulation and Experiment

Recently, simulations of mode converted IBW were performed with TORIC retaining up to 161 modes ($-80 \leq m \leq +80$) in the spectral expansion given in Eq. (1). These computations are seminal in nature because for the first time a spectral code has been used to resolve adequately IBW in toroidal geometry near $k_\perp \rho_{\rm i} \simeq 1$. Numerical resolution of the IBW is crucial for obtaining accurate estimates of electron Landau damping in mode conversion electron heating regimes. Analytic estimates of the required m-number for convergence of the spectral expansion can be obtained from $k_\perp \rho_{\rm i} \simeq 1$ with $k_\perp \simeq (m/r_{\rm mc})$, where $r_{\rm mc}$ is the radial location of the mode conversion layer [6]. An example of a large m−mode computation ($N_{\rm m} = 161$) is shown in Fig. 1 for a D(^{3}He) discharge in Alcator C-Mod. The plasma parameters in the simulation were $B_0 = 7.88$ T, $I_{\rm p} = 1170$ kA, $n_{\rm e}(0) = 2.4 \times 10^{20}$ m^{-3}, $n_{^3{\rm He}}/n_{\rm e} = 0.30$, $n_{\rm H}/n_{\rm e} = 0.05$, $n_{\rm D}/n_{\rm e} = 0.35$, $f_0 = 80$ MHz, $n_\phi = 10$, $T_{\rm e}(0) = 2.9$ keV, $T_{\rm D}(0) = 1.7$ keV, and $T_{^3{\rm He}}(0) = 1.7$ keV. For these parameters it is estimated that 240 poloidal modes or $-120 \leq m \leq +120$ would be required for absolute convergence of IBW at $k_\perp \rho_{\rm i} = 1$.

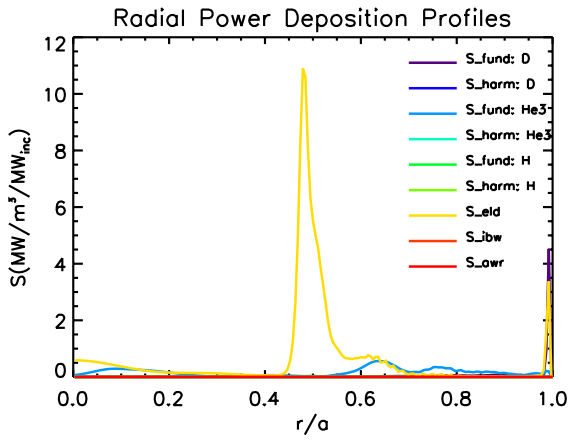

FIG. 1(a): Power deposition profiles for MCEH in C-Mod predicted by TORIC.

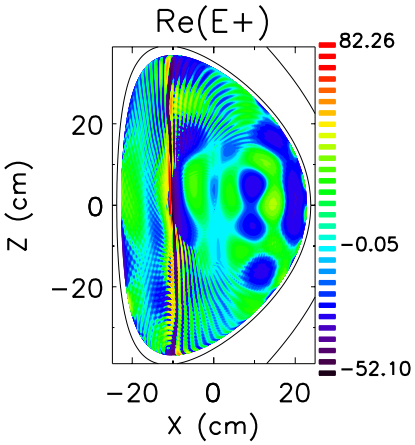

FIG. 1(b): Contours of $Re(E_+)$ for MCEH in C-Mod predicted by TORIC.

The integrated absorbed rf power due to fast wave and mode conversion electron heating in Fig. 1 is 70%, with most of the electron heating coming from the mode converted IBW. The fast wave power absorbed via fundamental ^{3}He cyclotron damping is 21%. The remaining 9% of the power is absorbed via fundamental deuterium cyclotron damping on the tokamak high field side. The importance of retaining enough poloidal modes in

these computations can be seen in Fig. 2, where the predictions of TORIC are compared with experimental measurements of MCEH from C-Mod. Clearly, using only 15 modes in the expansion (open diamond symbols in Fig. 2) results in a large underestimate of the electron heating at $n_{3_{\rm He}}/n_{\rm e} \gtrsim 0.2$. However, as the number of modes is increased to 161 in the 24% and 30% (^{3}He) cases, the TORIC predictions (solid diamonds) agree quite closely with the data. With too few poloidal modes, a Fourier reconstruction [using Eq. (1)] of the left circularly polarized electric field excited by the IBW will be grossly inaccurate on any flux surface passing through both the mode conversion layer and the ^{3}He cyclotron resonance [6], which in this case is a vertical chord through the plasma center in Fig. 1(b). This inaccuracy results in IBW absorption via ^{3}He cyclotron damping which is clearly not physical. Thus a sufficient number of poloidal modes insures that the IBW is well-localized near the mode conversion layer where it can only be absorbed via electron Landau damping [6].

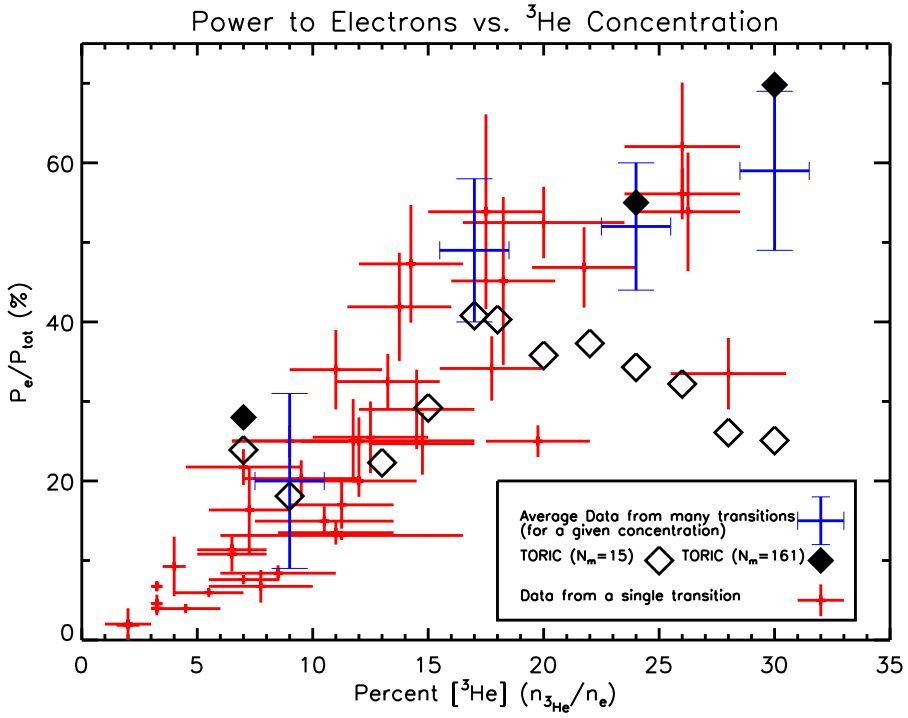

FIG. 2: Comparison of IBW Electron absorption from the C-Mod experiment with predictions of TORIC for $N_{\rm m} = 15$ (open diamond symbols) and for $N_{\rm m} = 161$ (solid diamond symbols).

2. TORIC-TRANSP Modelling of Internal Transport Barrier Mode

Recently an internal transport barrier mode was discovered in Alcator C-Mod using off-axis minority (H) cyclotron heating at 4.5 T [7]. A discharge exhibiting this barrier mode is shown in Figs. 3-4. In these plasmas the minority cyclotron resonance layer was located 9.6 cm to the high field side of the tokamak and approximately 2.5 MW of ICRF power at 80 MHz was injected through two separate dipole antennas. The RF power was injected at 0.7 s and the density profile started to peak at about 0.95 s. The plasma enters an H-mode phase after the rf is turned on and remains in H-mode throughout the density peaking. Interestingly, the central toroidal plasma rotation (Fig. 3)

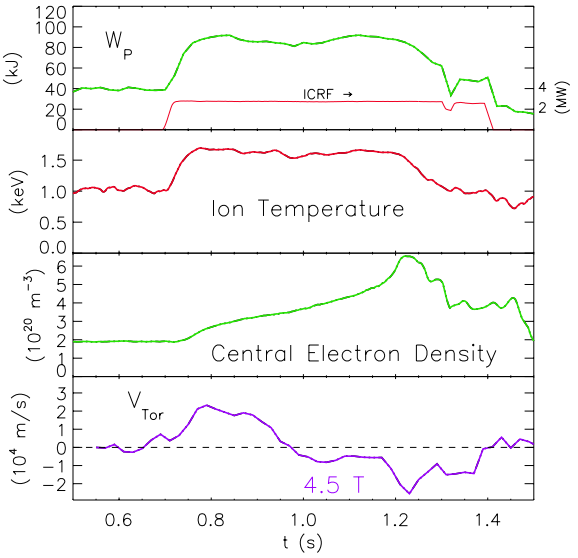

FIG. 3: ICRF-induced ITB mode in C-Mod at 4.5 T.

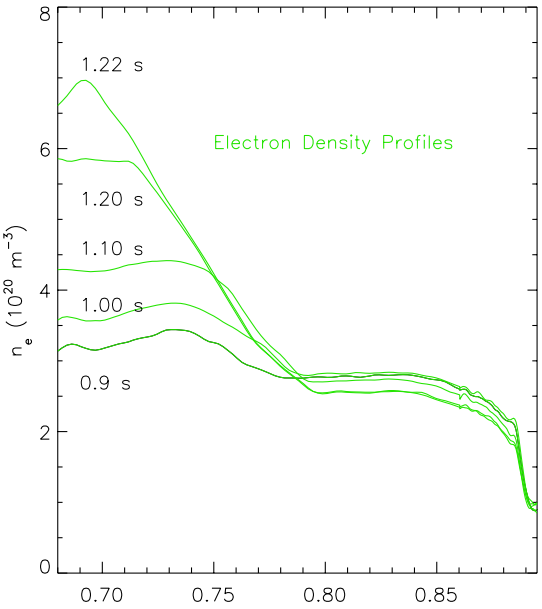

FIG. 4: Formation of barrier in density profile for discharge in Fig. 3.

slows down as the density profile peaks and eventually reverses direction from co-current to counter-current [8]. The toroidal rotation velocities in Fig. 3 were determined from the Doppler shifts of the Ar^{17+} Lyman α doublet [8]. The electron density profiles were determined from visible bremsstrahlung measurements and the central ion temperature was inferred from the measured neutron flux. The stored energy inferred from an EFIT reconstruction of the MHD equilibrium based on magnetic loop measurements is also shown in Fig. 3 and remains relatively constant. The electron temperature profile is measured by a six channel Thomson scattering system and the temporal evolution of $T_e(0)$ was found to be very close to $T_i(0)$.

This discharge was analyzed using the transport analysis tool TRANSP which was recently coupled [9] to the TORIC ICRF module through the Fokker Planck package FPPRF. T_i profile data from the high resolution X-ray spectroscopy diagnostic (HIREX) [8] were limited to only a few points within $r/a \lesssim 0.5$ in these plasmas. Thus the TRANSP analysis was performed assuming an ion diffusivity of the form $\chi_i = M_i \chi_i^{CH}$, where χ_i^{CH} is the ion conductivity of Chang-Hinton. The multiplier (M_i) was adjusted to predict a T_i that would yield a computed neutron flux to match the experimentally measured value. The ICRF power deposition profiles at 1.0 s predicted by TORIC and FPPRF are plotted in Fig. 5. About 2.4 MW of incident fast wave power was absorbed via minority (H) cyclotron damping at $r/a \simeq 0.4$. A small fraction of the incident wave power was absorbed via direct electron Landau damping of the fast wave near the plasma center. As the fast ion tail slows down collisionally at this time, about 1 MW of the tail power equilibrates on background deuterons and 1.4 MW slows down via electron drag. The density barrier in Fig. 4 is not seen in ICRF heated plasmas until B_0 is reduced to 4.5 T or lower. This moves the ICRF minority resonance at least 9.6 cm to the high field side at a mapped major radius of $R \simeq 0.76$ m. This major radius also corresponds to the approximate location where the density barrier forms in Fig. 4. A direct causal link between the presence of ICRF heating power and the formation of the

density barrier cannot be concluded, however since this type of barrier is also observed in ohmic H-mode plasmas in C-Mod [8].

The effective diffusivity ($\chi_{\rm eff}$) computed by TRANSP for this discharge is plotted versus time in Fig. 6 for one radial location well within the density barrier ($r/a = 0.05$) and for one location outside the barrier ($r/a = 0.6$). The temporal behaviour of $\chi_{\rm eff}$ suggests the formation of an ITB as $\chi_{\rm eff}$ drops by a factor of 2-3 within the barrier region and remains relatively unchanged outside. Future experiments are planned at low field ($B_0 \simeq 4.1 - 4.5$ T) to investigate the potential of this barrier mode as a target plasma in advanced tokamak studies in Alcator C-Mod. In these experiments ICRF power at 80 MHz will be injected again to induce the density barrier and tunable ICRF power at 70 MHz will be used to raise simultaneously the plasma temperature on-axis.

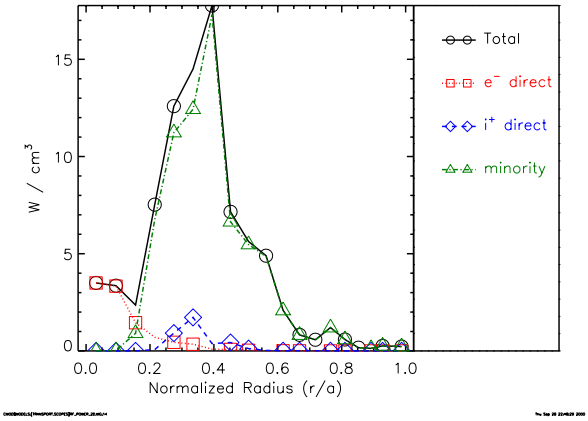

FIG. 5: ICRF deposition profiles from TORIC - TRANSP analysis of the C-Mod discharge in Fig. 3

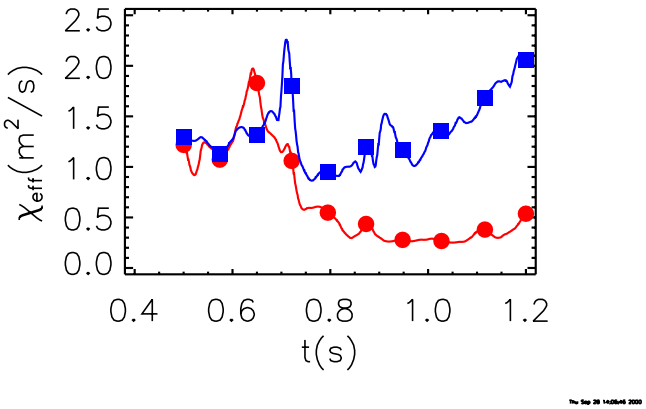

FIG. 6: $\chi_{\rm eff}$ versus time from TRANSP analysis of C-Mod discharge in Fig. 3. Trace with square symbols corresponds to $r/a = 0.6$ and trace with circles corresponds to $r/a = 0.05$

*Work supported by the US Department of Energy Contract No. DE-FC02-99ER54512.

[1] Hutchinson, I.H. et al., Phys. Plasmas **1**, (1994) 1511

[2] Brambilla, M. and Krücken, T., Nucl. Fusion **28**, (1988) 1813.

[2] Brambilla, M., Nucl. Fusion **38**, (1998) 1805.

[4] Hammett, G.W., PhD Dissertation, University Microfilms International No. GAX86-12694, Princeton University (1986).

[5] Hawryluk, R., in Physics of Plasma Close to Thermonuclear Conditions, (Varenna, 1979), Commission of the European Communities, Brussels, Vol. I, p. 61 (1979).

[6] Bonoli, P.T., et al., Phys. Plasmas **7**, (2000) 1886.

[7] Wukitch, S.J. et al., 27^{TH} EPS Conf. on Contr. Fusion and Plasma Physics, Budapest, (June, 2000), paper p3.105 (to be published).

[8] Rice, J.E., et al., 18^{TH} IAEA Fusion Energy Conference, (Sorrento, Italy), paper IAEA-CN-77 EXP 5/24; submitted to Nuclear Fusion.

[9] Phillips, C.K., et al., US - Japan Workshop on Radio Frequency Physics, March 14-16, 2000 (Plasma Physics Laboratory, Princeton, NJ).